Available online at www.joac.info

ISSN: 2278-1862

Journal of Applicable Chemistry

2017, 6 (6): 1058-1068

(International Peer Reviewed Journal)

Synthesis and Microstructural Characterization of Modified Nano-Cerium Silica Mesoporous by Surfactant-Assisted Hydrothermal Method

Gusliani Eka Putri[1], Syukri Arief [2], Novesar Jamarun[2*], Feni Rahayu Gusti[1], Adel Fisli[3], Zilfa[2] and Upita Septiani[2]

1. The Insitute of Health Science Syedza Saintika, Padang, West Sumatera, **INDONESIA**
2. Department of Chemistry, Faculty of Mathematics and Science, Andalas University, Padang, West Sumatera, **INDONESIA**
3. Center for Technology of Nuclear Industry Materials, National Nuclear Energy Agency, Kawasan Puspiptek, Serpong, **INDONESIA**

Email: novesar62@yahoo.com

Accepted on 13th October 2017, Published online on 27th November 2017

ABSTRACT

Mesoporous silica modified doped nano crystalline cerium oxide (Ceria) has been successfully synthesized by the surfactant-assisted hydrothermal method. The surfactant was used cetyltrimethylammonium bromide (CTAB), tetraethyl orthosilicate (TEOS) was used as a source of silica, cerium nitrate hexa hydrate was used as a cerium source. The comparison of Si/Ce mole is 10 with hydrothermal condition 368^oK*. Mesoporous silica that is already formed modified with acid Lewis and base Bronsted was Iron (III) chloride and Aniline to increase catalyst activity. The effect of the hydrothermal method showed the at the material produced had a high surface area (~500-700* m^2g^{-1}*), narrow pore diameter (~ 2,76-11,74 nm), large of pore volume (~ 0,27 - 1,58 cc* g^{-1}*) and uniform of pore indicated by* N_2 *adsorption desorption, transmission electron microscopy (TEM) and scanning electron microscopy (SEM) data. The result of wide angle X-ray diffraction (XRD) showed a specific peak of* 2θ *mesoporous silica between 20-25* ^{o}*. The success of the cerium doping process into the mesoporous silica (MS) and modified mesoporous silica (MMS) pore framework can be seen from the Fourier transform infrared (FTIR) results with the appearance of a new peak and a peak absorption shift. The number of cerium has been doped on MS and MMS as much as 33,131% (MS) and 35,169% (MMS) which can be seen from X-Ray Fluorescence (XRF) analysis. The optical photocatalytic properties tested were analysed by diffuse reflectance UV-visible spectroscopy (DRUV-vis) showed the MMS-Ce light absorption wider than MS-Ce and Ceria so that light capture was more efficiently used as a photocatalyst. Of all the tests that have been done can be concluded that the doping cerium with MMS photocatalysis properties better than doping cerium to MS.*

Graphical Abstract

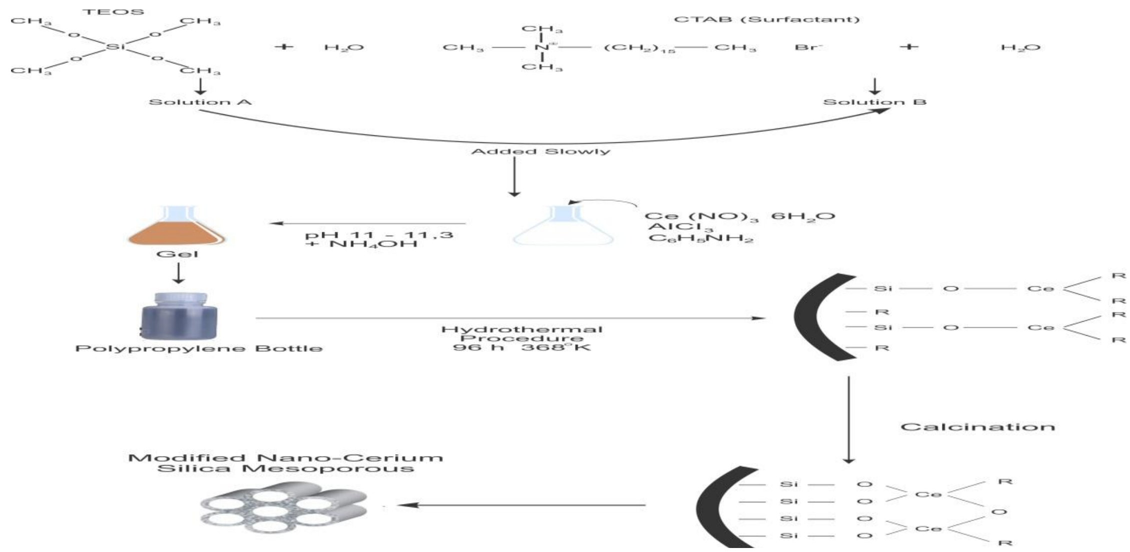

High Lights

- Modified nano –cerium silica mesoporous were synthesized by surfactant-assisted hydrothermal Method.
- Encapsulation Cerium in framework modified mesoporous silica was capable of increasing material reactivity.

Cetyltrimethylammonium Bromide (CTAB) (Surfactant) is used to decrease surface pressure, interface tension, increasing dispersed particle stability, and controlling emulsion formation characteristic.

Keywords: Mesoporous, Nanocrystalline, Cerium Oxide, hydrothermal.

INTRODUCTION

Cerium oxide is grouped into rare earth metal. For the past few years, oxide nano material attracts many researchers due to its good mechanical, electrical, optical, and catalyst feature. Cerium oxide (CeO_2) is known as Ceria. Ceria is a popular oxide nano material widely used in industrial sector because Ceria has low refractive index, high oxidation power, energy band gap of 3,2 eV, very sensitive towards visible light, and low absorption toward Ceria UV which had nano structure and better at absorbing UV light [1,2]. Ceria nano particle role in absorbing UV light is enhanced through decreasing crystallite size In this study, cerium oxide is doped with modified mesoporous silica. Mesoporous silica has wide surface area, regular structure and homogenous cavity with homogenous pores. Cerium oxide doped with mesoporous silica is expected to enhance cerium oxide photocatalytic activity thus becoming more optimum if used as photocatalyst [3,4].One alternative method that is easy to implement is a method of using the compound photocatalyst photodegradation using oxide nanomaterial. So far, nano material oxides are widely publicized in the process of degradation of dye is titanium oxide (TiO_2) [5,6,7]. However, titanium oxide material is expensive and unstable photocatalytic activity in various forms of crystal structure. Oxide nanomaterial that many researchers draw attention to the last few years because it has properties of mechanical, electrical, optical and catalytic properties are good, namely, cerium oxide (CeO_2) commonly known as Ceria.

In this study, cerium oxide nano crystalline was synthesized using hydrothermal method. Hydrothermal method has several superiorities such as relatively lower temperature, producing particles with high crystallinity, high purity, and homogenous particle size [8]. Hydrothermal method is modified with adding surfactant. Surface active substance known as surfactant is an active compound, lowering the surface tension and has bipolar structure. The head part is hydrophilic and the tail is hydrophobic, so surfactant stays between two different polarity phase and hydrogen bound, for example oil and water. Surfactant is used to decrease surface pressure, interface tension, increasing dispersed particle stability, and controlling emulsion formation characteristic. One of the example of surfactant is CTAB. CTAB in the solution is ionized into CTA^+ and Br^-. Hydrophilic end or known as head consists of ammonium complex and hydrophobic end or known as tail consists of hydrocarbon chain composed of ethyl group. With adding CTAB, particles might have better photocatalytic feature [9].

MATERIALS AND METHODS

Chemicals and Reagents: TEOS (Tetraethyl Orthosilicate), acetate acid (CH_3COOH), aniline ($C_6H_5NH_2$), Iron (III) Chloride, Cetyltrimethylammonium Bromide (CTAB), Ammonium hydroxide (NH_4OH), water (aquods), toluene, methanol, $Ce(NO_3)_3$,.$6H_2O$ (Cerium Nitrate Hexahydrate), pure isopropanol (MERCK)

Material Synthesis: Ratio of silica: cerium Oxide (CeO_2): CTAB (Cetyltrimethylammonium Bromide) : Nh_4OH : H_2O is 0,025 : 0,0005 : 0,00625 : 5,55 (Vargas et al., 2013). Mesoporous silica with ratio between Si/Ce = 10 was made with surfactant-assisted hydrothermal through sol-gel process. As much as 5,54 mL TEOs was mixed with 50 mL aquods (solution A). Then, solution A was stirred for 30 minutes. Meanwhile, solution B was made with mixing 2.28 g CTAB with 50 mL aquods. Solution B was stirred for 30 min. Solution A was poured slowly into solution B, and stirred. Then, mixture of solution A and B was stirred for 24 h until gel was made. Ceria synthesis was made with dissolving Cerium Nitrate Hexahydrate into aquods solvent and isopropanol with ratio of 1: 6 and ammonium hydroxide was added slowly until it reaches pH of 9 while stirred. Then refluxed for 30 minutes and filtered until yellow precipitate/sediments was obtained. This yellow sediment then washed with isopropanol and dried off for 5 h in 60 ^{o} C, until yellow powder was obtained. Yellow powder was added into the gel and stirred for 1 h and ammonium hydroxide was added and stirred until pH of 11-11,3, then light yellow suspension was made. Let suspension sit for 12 h. Suspension was added into polypropylene bottle (PP) and warmed up with temperature of 368^o K for 96 h so white-yellowish sediment was formed. This sediment then calcined in temperature of 623 ^{o} K for 4 h and continued in 873 ^{o} K for 4 h so Mesoporous Silica-Cerium (MS-Ce) was formed.Modification of silica was done by adding Acid Lewis (iron (III) chloride) and base Bronsted (aniline) so Modified Mesoporous Silica -Cerium Mesoporous Silica (MMS-Ce) was formed.

Characterization: Structure of cerium oxide nano crystalline was tested with X-ray Diffractions (XRD) meanwhile crystal size was analysed based on full-width-half-maximum (FWHM), each of the peak was diffracted with X ray using Williamson-Hall equation. Pore diameter and surface area of crystal were analyzed using N_2 absorption desorption. Micro structural analysis was done using SEM and TEM. Forming composition was characterized with XRF.

RESULTS AND DISCUSSION

N_2 adsorption measurement: Result of N2 adsorption measurement was analyzed using DFT (Density Functional Theory) method. Mesoporous size analysis was based on application of Kelvin equation using Barret, Joyner, and Halenda (BJH) method. But Kelvin equation resulted in less accurate result in analysing mesoporous size < ~ 10 nm [9]. Kelvin equation limitation can be solved with DFT method. DFT method analyses micro and meso surface absorption in molecular stage based on statistic mechanism. DFT uses complex mathematical model and illustrates interaction gas-solid and gas-gas (gas-liquid) and supported with geometrical analysis (pore geometry). Pore size distribution is more accurate using DFT analysis. DFT method presents information regarding to absorption and desorption from hysteresis loop and predicts condensation and hysteresis pore characteristic quantitatively by calculating underlying absorption [10]. Based on that, DFT method was used in pole diameter and pore volume measurement. DFT analysis results of the resulting material can be seen from Table 1.

Table 1. Texture characteristic from produced material

Material	**S_{DFT}(m^2 g $^{-1}$)**	**$V_{p/po\ \sim 1}$ (cc g-1)**	**D $_{DFT}$ (nm)**
CeO_2	73,5	0,27	11,74
SM	674,4	1,58	2,76
SM-Ce	531,2	1,04	3.03
SMM	599,6	1,06	3,17
SMM-Ce	465,1	0,89	3,03

Table 1 showed increasing of material surface area and pore volume after cerium oxide encapsulation on mesoporous silica surface (MS). Surface area increased from 73,5 to 531,2 and pore volume increased from 0,27 to 1,04. When cerium oxide was encapsulated on modified mesoporous silica surface (MMS), surface area increased from 73,5 to 465,1 and pore volume increased from 0,27 to 0,89. After Ceria encapsulation on mesoporous silica, pore diameter became smaller. Pore diameter decreased from 11,7 to 3,03 (MS-Ce and MMS-Ce). The smaller pore diameter, the particle size become smaller. The smaller the particle, the reactivity increases due to increasing surface area that causes more atomic fraction on the surface, more atomic fraction on the surface leads to increasing material reactivity [8].

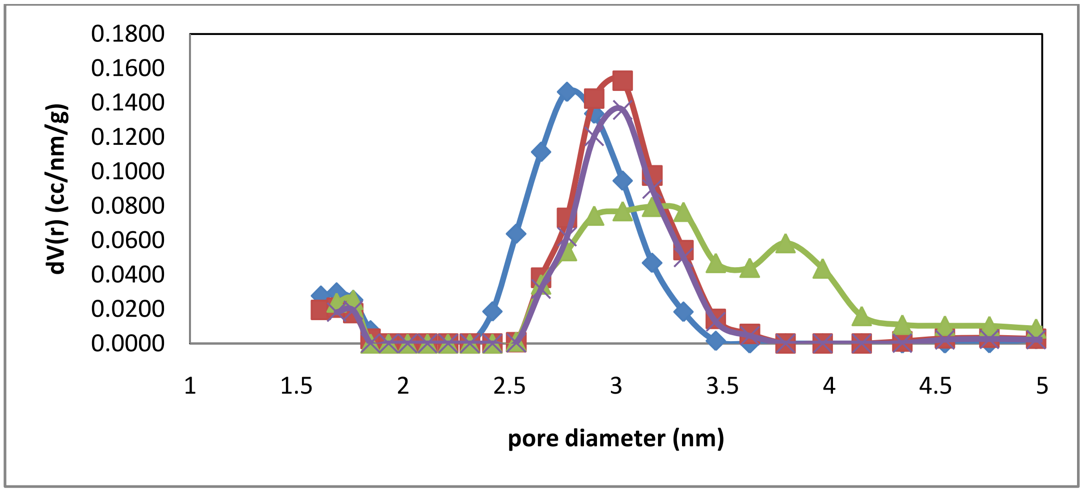

Figure 1. Comparison of DFT pore diameter of Mesoporous Silica (MS), Modified Mesoporous Silica (MMS), Mesoporous Silica- Cerium (MS-Ce), Modified Mesoporous Silica-Cerium (MMS-Ce)

Figure 1 showed the curve with parallelogram marking as the pore diameter curve from observable MS pore diameter which was 276 nm. MS pore diameter while it was doped with Cerium was shown by the curve with rectangular marking. MS-Ce curve was shifted and the pore diameter was 303 nm. Curve with triangular marking was the pore diameter of MMS. Pore diameter of MMS was not homogenous because therewas more than one peak. However, when MMS was doped with cerium, pore diameter was more homogenous, indicated by the pore diameter peak with *X* sign only had one peak.

XRD analysis: XRD test was done to obtain crystal size from each sample. Peak intensity of Cerium oxide (CeO_2) absorbed in the angle of 2 θ was28,7^o, 33,2 ^{o}, 47,5 ^{o}, 56,7 ^{o}, 59,2 ^{o}, 69,5^o , 76,8 ^{o}, 79,1^o, 88,3 ^{o} and 95,5 ^{o}. The crystal lattice was (110), (200), (220), (311), (222), (400), (331), (420), (422), and (511) based on JCPDS standard No. 00-043-1002. Peak intensity of MS and MMS that were absorbed at the angle of 2 θ was 23,5 ^{o} and 24,5 ^{o}. This result was in accordance with Bing et al., 2011, argued that mesoporous silica (MCM-41) had specific peak at the angle of 2θ between 20-15 ° based on Wide Angle XRD analysis. If small angle XRD analysis was conducted, the peak was obtained at 2θ, 3,8 ° (110) and 4,4 ° (200) with weak intensity. When Ceria was encapsulated on MS and MMS pore, silica *amorf* peak was covered by Ceria so thus crystal absorbed at 2θ was shifted from the Ceria 2θ peak absorption shawn in figure 2.

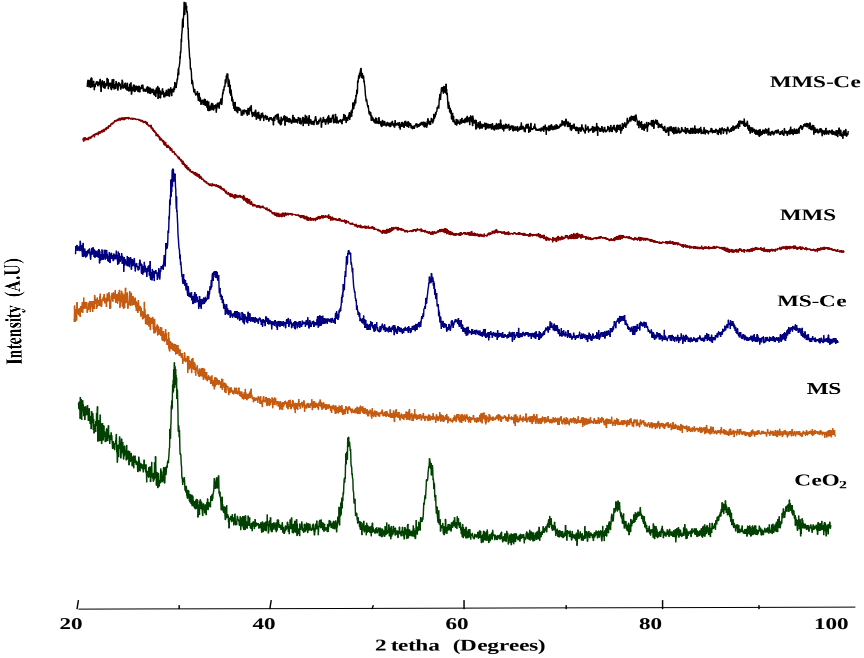

Figure 2. Comparison of Wide Angle XRD of Mesoporous Silica (MS), Modified Mesoporous Silica (MMS), Mesoporous Silica- Cerium (MS-Ce), Modified Mesoporous Silica-Cerium (MMS-Ce)

Small size crystallites resulted in very wide diffraction peak. Diffraction peak width produced crystallites size information. The wider the X ray diffraction peak, the smaller the crystallites. Diffraction peak was produced by interfering of reflected light by crystal surface. Correlation between crystallites size and X ray diffraction peak was measured with Scherrer equation [12-14]

$$\beta = \frac{FWHMLeft\ [°2\ Th]*\pi}{180} \tag{1}$$

$$D = \frac{k\lambda}{\beta Cos\theta} \tag{2}$$

As in equation (1) and (2)Where D is Crystallite site (in nm), B is FWHM (line broadening at Half the Maximum intensity), the value is obtained by subtracting FWHM value with the instrumental line broadening (in radian), 2θ is Bragg’s Angle, λ is X ray wave length, and K is the constants of the shape factor (0,8-1). Result of XRD CeO_2, MS-Ce and MMS-Ce showed narrowing X-ray diffraction peak, therefore big sized crystal was produced. Cerium oxide crystal size was 1,04-99,19 nm, MS-Ce crystal size was 10,88- 31,70 nm and MMS-Ce crystal size was 10,48 - 98,23 nm. Nano crystalline was defined as a crystal particle with size smaller than 100 nm. Based on crystal size measurement, it was shown that all crystal size smaller than 100 nm indicated success synthesis process. Cerium oxide nano crystalline was successfully synthesized with range of size from 11,04 to 99,19 nm.

DRS-UV Visible Analysis: In this study, measurement was done with 200-800 nm wavelength. Radiation for UV was about 180-380 and for visible light was 380-780 [13]. Result of DRS UV-Vis analysis is shown in figure 3, dotted line showed absorption result from cerium oxide photocatalyst. It showed that absorption of cerium oxide nano crystalline in the 200nm wavelength, 245 nm, and 290 in absorption area ended at the wavelength of approximately 500 nm, which was part of the visible area. Curve with dotted line showed absorption of MS-Ce. Photocatalyst MS-Ce absorption area with wavelength of 125 nm, 275 nm, 305 nm, 325 nm, and 365 nm and absorption area ended in wavelength of approximately 600 nm, which was the visible area. Absorption of DRS UV-Vis MMS-Ce is shown by black line. Absorption area of photocatalyst MMS-Ce at the wavelength of 200 nm and 275 nm and absorption area ended at the wavelength of 750 nm, which was the visible area. Visible light with spectrum of 400 nm and 700 nm wavelength was 45% of total sun radiation energy, meanwhile UV light was less than 10% [15]. Based on that, it is very interesting to increase photocatalytic activity in application photocatalytic on visible light. Based on absorption of DRS UV-Vis, it was concluded that the resulted photo catalyst had wide range of absorption, and include the visible light so thus Ceria, MS-Ce, and MMS-Ce photocatalyst was suitable as photocatalyst with sunlight support because the absorption area could reaches visible area.

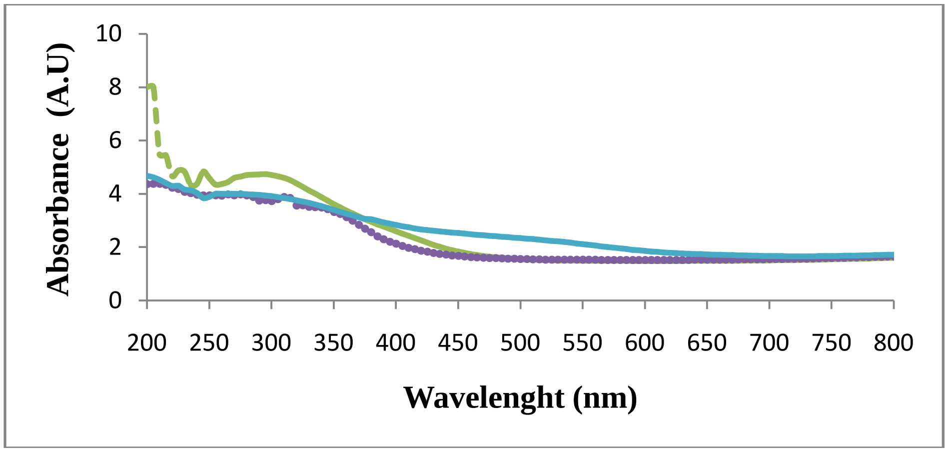

Figure 3. Comparison result DRS UV-Vis of Mesoporous Silica- Cerium (MS-Ce), Modified Mesoporous Silica-Cerium (MMS-Ce)

FTIR Characterization: FTIR is used to identify material, determine composition of a substance mixture, and obtaining information in order to estimate molecular structure. Sample is usually solid, liquid, or gas material. Figure 4 showed spectrum FTIR from (a) Cerium oxide (B) Mesoporous silica (MS) (c) Mesoporous Silica -Cerium (MS-Ce) (d) Modified Mesoporous Silica (MMS) and (e) Modified Mesoporous Silica-Cerium (MMS-Ce)**.** Spectra FTIR from MCM-141 had four specific bands absorption presented as wave number of 456, 796, 957, and 1085. Wave number of 961 cm^{-1} showed absorption band of Si-O-Si Group which was estimated as the absorption band with MCM-141 characteristic [17]. Result of FTIR from MS (b) MMS (d) showed similar absorption pattern, but shifted of the absorption band was present. Vibration band on wavelength of 400-600 cm^{-1} showed Si-O-Si bond bending (δ) [16] on the peak MS appear in the wavelength about 471 cm^{-1}, on MMS about 577 cm^{-1} showed Si-O-Si bending vibration from SiO_4 structure. Vargas et al, 2012 [18], and Munusamy et al, 2013 [19], argued that $_{\delta}$ (Si-O-Si) vibration appears on the wavelength of 464 cm^{-1} and 470 cm^{-1}. Absorption band on wave number of approximately 790-812 cm^{-1} was the Si-O-Si stretching vibration ($_{v}$) [12] on this peak MS appeared on the wave number of approximately 805 cm^{-1}, shifting of wavelength 801 cm^{-1} occurred in MMS. Vargas et al, 2012 [18] and Munusamy et al, 2013 [19] stated that$_{Vs}$(Si-O-Si) peak appears on wave number of approximately 802 cm^{-1} and 800 cm^{-1}.

Absorption band in wave number of 1130-1000 cm^{-1} was as asymmetrical Si-O-Si $_{Vas}$ (Si-O-Si) vibration band [16], on MS the peak the vibration occurs in wave number of 1060 cm^{-1}, on MMS 1059 cm^{-1} wavelength shifting occurred. Vargas et al, 2012 [18] and Munusamy et al, 2013 [19] argued that the peak of $_{Vas}$ (Si-O-Si) occurred at wave number of approximately 1090 cm^{-1} and 1090 cm^{-1}. Wide absorption band on area approximately 3500 cm^{-1} and absorption band approximately 1600-1800 cm^{-1} [16] were the result of stretching vibration (v) and water molecules bending (δ) with Si-OH bond (silanol). The $_{VOH}$ (Si-OH) MS vibration and $_{\delta OH}$(Si-OH) were formed on the wave number of approximately 3414 cm^{-1} and 1635 cm^{-1}, on MMS there was a shift on wavelength of 3657 cm^{-1} and 1852 cm^{-1}, this indicated silanol group existence in the silica framework pores system. Vargas et al, 2012 [18] stated that $_{VOH}$(Si-OH) and $_{\delta OH}$(Si-OH) vibration occurred in the wave number of approximately 3422 cm^{-1} and 1633 cm^{-1}. Munusamy et al, 2013 stated $_{VOH}$(Si-OH) and $_{\delta OH}$(Si-OH) vibration occurred on the wave number of approximately 3440 cm^{-1} and 1635 cm^{-1} [19].

FTIR and MMS absorption spectrum underwent transformation from MS spectrum and had additional new peak in the wave length of 14831 cm^{-1}, this indicated the existence of aromatic C-N stretching from aniline. Absorption in the wavelength of 1560-1530 cm^{-1} indicated the vibration band of primary amine from NH_2 bond on MMS peak occurred at the wavelength of 1532 cm^{-1}. Absorption on the wavelength of 2200-2000 cm^{-1} showed combination of stretching N-H vibration and stretching OH on the peak of MMS that occurred on wavelength of 2171 cm^{-1}, this indicated N-H stretching vibration and OH stretching from aniline molecules and water. Symmetrical primary amina band vibration occurred on the wavelength of 3190-3170 cm^{-1}, on MMS that peak occurred on the wave length of 2171 cm^{-1} and this indicated symmetrical primary amine bond from aniline which was categorized as primary amine.

Absorption spectrum of FTIR Ceria nano particle on the wavelength of 770 cm^{-1} indicated Ce-O stretching bond [20]. Figure 4(a) showed on the wavelength of 701 cm^{-1}, where the peak of Ce-O from CeO_2 nanoparticle emerged. On the wavelength of 3500 cm^{-1} and 1541 cm^{-1}, OH vibration peak and bending vibration between H_2O and CeO_2 nanoparticle emerged.

MS-Ce FTIR spectrum and MMS-Ce were similar with MS FTIR spectrum and MMS but had minor peak shifting, decreasing peak intensity on several missing peaks. Absorption of Ce-O stretching bond occurred in the wavelength of 400-600 cm^{-1} and indistinguishable with bending vibration (Si-O-Si). Vibration of$_\delta$(Si-O-Si), v_s(Si-O-Si), v_{as}(Si-O-Si), v_{OH}(Si-OH) andδ_{OH}(Si-OH) on MS and MMS underwent wavelength shifting caused by electro positive Cerium ion encapsulation on electro negative oxygen atom on mesoporous silica nano particle.

All FTIR absorption spectrum result above showed that the success of the Ceria encapsulation process on modified mesoporous silica nano particle and this lead to Ceria growth on modified mesoporous silica nano particle surface. Ceria nano crystalline growth on the silica surface happened because covalent bound between Ceria and Silica and this formed Cerium-Silicate bond. This process was supported by experimental observation result where the white solution color turn into clouded (hydroxide) and yellowish (oxide).

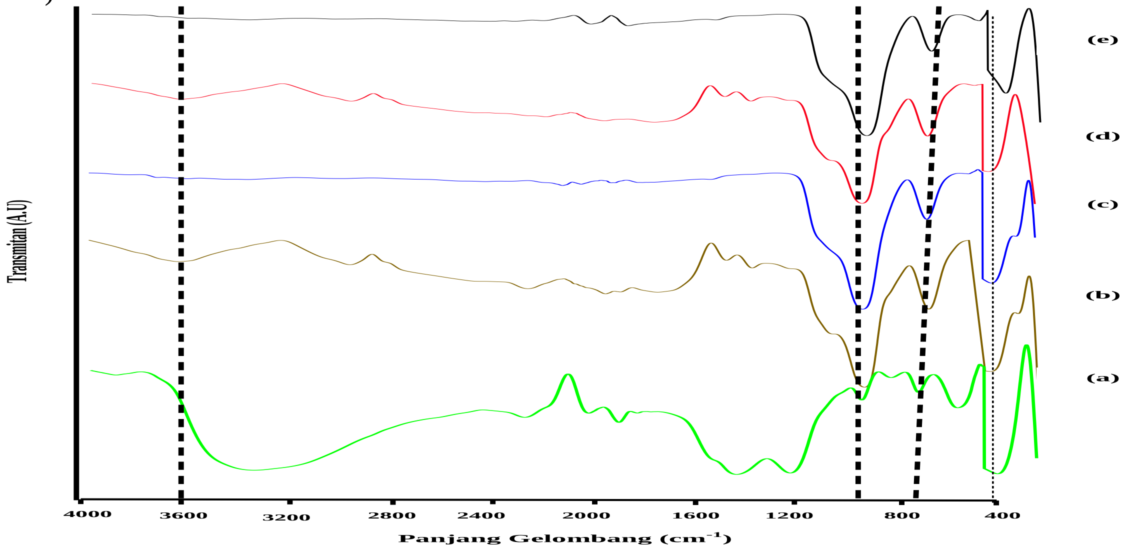

Figure 4. Comparison FTIR resultsof (a) cerium Oxide (b) Mesoporous Silica (MS), (c) Mesoporous Silica-Cerium (MS-Ce), (d) Modified Mesoporous Silica (MMS), and (e) Modified Mesoporous Silica-Cerium (MMS-Ce)

Morphological Features: Morphological analysis was done using SEM and TEM. Result from cerium oxide (a) showed round shaped particle with homogenous size. TEM and SEM analysis on MS-Ce samples showed round shaped particles with well-ordered hexagonal arrangement. However, samples of MMS-Ce, the arrangement of the pore systems became more ordered. On the TEM MS-Ce and MMS-Ce pictures, it showed dark area representing Cerium oxide (Ceria) which was successfully encapsulated into mesoporous silica with hexagonal shaped pores (b) and (c). TEM analysis also revealed that Ceria nano particle was distributed onto mesoporous silica surface. This was in accordance with Huang et al, 2012, found hexagonal pore structure on mesoporous silica [21]. Doped cerium into mesoporous silica causes structural regularity, this data was supported with DFT pore analysis in Figure 5.

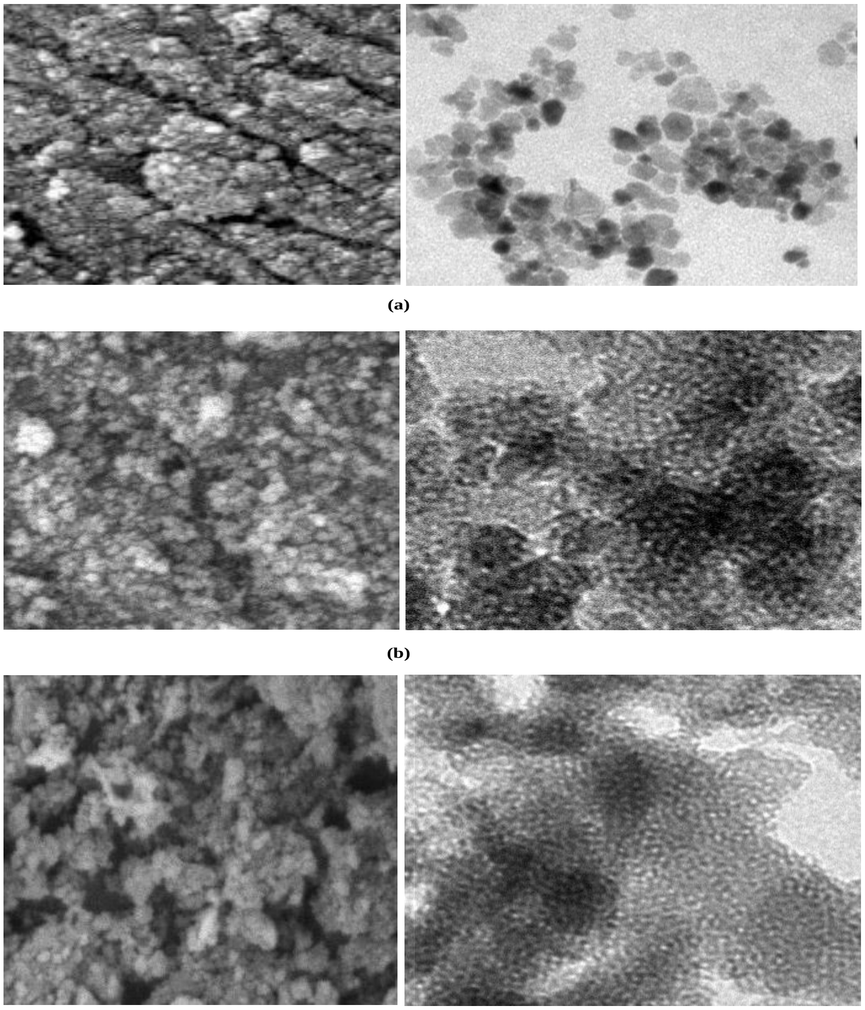

(a)

(b)

(c)

Figure 5. The results of SEM analysis (left) TEM (right) (a) of Cerium Oxide (b) mesoporous silica-cerium (MS-Ce) and (c) Modified mesoporous silica - cerium (SMM-Ce)

XRF Analysis: XRF (X-ray fluorescence spectrometry) is a non-destructive analysis technique to identify and locate element concentration in a solid, powder, or liquid. XRF method is widely used to determine element composition of a material. XRF is a quick method and doesn't damage sample, this method was chosen in the field application and industrial area to control the materials [22].

Figure 6 showed MS,MMS, CeO_2 (Ceria), MS-Ce, and MMS-Ce were successfully synthesized, and decreasing composition of Si in MS shape, with total of 98,518% while forming MMS composition % unit Si decreasing to 84,346%. While Ceria was encapsulated into Silica composition % unit Si pores into 65,187% (MS-Ce), decreasing Si unit % occurred because 33,131% Ceria enter silica pores so thus Si composition was decreasing, this indicated a succeed Ceria encapsulated process on MS support. Meanwhile, Si unit % composition on MMS while encapsulated by Ceria was decreasing to 55,412% (MMS-Ce) the encapsulated Ceria was 35,169% and the remaining was from Lewis acid ($FeCl_3$) as much as 7,392%. Lewis acid was used to activate MS surface so thus MMS was formed. $FeCl_3$ was used as Lewis acid and aniline was used base Bronsted.

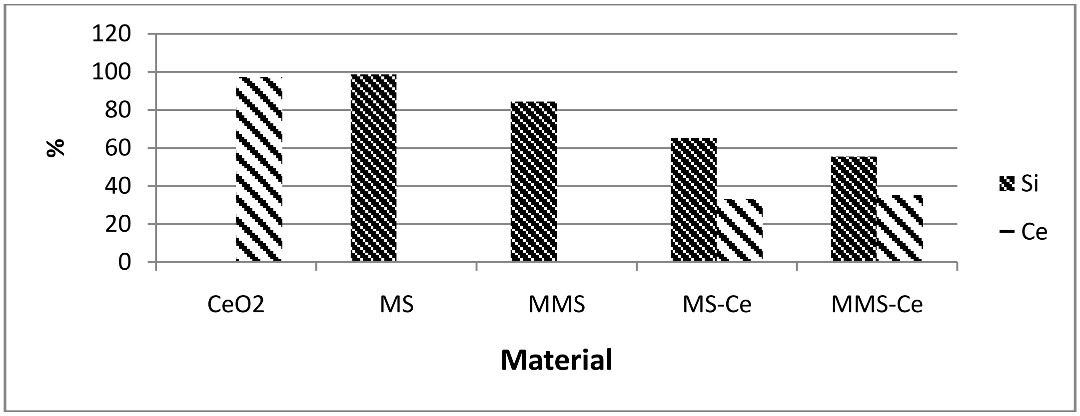

Figure 6. The Comparison analysis XRF of Ceria, MS, MMS, MS-Ce and MMS-Ce

APPLICATIONS

The Synthesized of material contains silica in the frame work and cerium, acid Lewis and base Bronsted on the surface of material. Photocatalytic activity is used to degrade the methylene blue dye. The purpose of this study was to produce a new photocatalyst by means of ceria doped with silica which is expected have high reactivity to decompose hazardous dyestuff waste.

CONCLUSIONS

Mesoporous silica synthesis (MS), Modified Mesoporous Silica (MMS) and Ceria nano crystalline was successfully synthesized, indicated by N_2 absorption desorption result where the surface area value $_S$DFT , SM, SMM, and Ceria were 674,4 m^{-2} g^{-1},599,6 m^{-2} g^{-1} and 73,5 m^{-2} g^{-1}, respectively, with pore diameter of 2,76 nm, 3,17 nm, and 11,74 nm, respectively. Ceria nano crystalline encapsulated process on modified mesoporous silica was proven with UV-Vis test where MS-Ce and MMS-Ce had absorption on UV and the visible light area. Data was supported with TEM and SEM test which showed Ceria entered silica pores cavity structure.

ACKNOWLEDGEMENTS

Thanks to the directorate of research and community service of Indonesia (DRPM) KEMENRISTEKDIKTI has been funded this research. Thanks to KOPERTIS X who has built us and the institute of health science SYEDZA SAINTIKA.

REFERENCES

[1] E.Toni, A.M.Yin, Shu, S. Tsugio, *Journal Mater Science*, **2013,** 43, 2411-2417.
[2] Y. Minamidate, S.Yin, T.Sato, *Materials Chemistry and Physics Scince Direc*, **2010**, 516-520.

[3] S. Arief, *Research of Journal Pharmaceutical, Biological and Chemical Science*, **2015**, 6, 1511-1518.
[4] N. Jamarun, *Research Journal of Pharmaceutical,Biological and Chemical Science*s, **2015**, 6, 3.
[5] A.F. Reji, N.R. Alphonse, *J. Applicable Chem*, **2013**, 2(2), 311-316.
[6] A. Paliwal, R.Banu, R. Ameta, S.C Ameta, *J.Applicable Chem*, **2017**, 6(5), 967- 975.
[7] Fayed, Alkaim, M.B. Alqaraguly, *J. Applicable Chem*, **2013**, 2(2), 291-303.
[8] J.Rouquerol, P.Sing, G.Lewellyn, Maurin, *Adsorption by Powders and Porous Solids: Principles, Methodology and Applications*, **2014**, Academic Press, 2nd edition, 646.
[9] J.Landers, G.Y.Gor, A.V. Neimark, *Journal Colloids and Surfaces A: Physicochemical and Enginee ring Aspects*, **2013**, 437, 3-32.
[10] L. Almar a, A. Tarancóna, T. Andreua, M. Torrell, Y. Hub, G. Dezanneaub, A. Morata, *Sensors and Actuators B*, **2015**, 216, 41-48.
[11] T.Xie, X.Zhao, Zhang, J.Shi, D.Zhang, *Internasional Journal of Hydrogen Energy*, **2015**, 40, 9685-9695.
[12] S.Kozhukharov, Z.Nenova, T.Nenov, N.Nedev, M.Machkova, *Sensors and Actuators B: Chemical*, **2015**, 210, 676-684.
[13] J. Jagiello, J. Kenvin, J. Olivier, A. Lupini, C. Contescu, *Journal Sci. Technol*, **2011**, 29, 769–780.
[14] M. Nookaraju, A.Rajini, I.A.K Reddy, *Journal of Applicable Chemistry*, **2013**, 2(2), 122-128.
[15] G.Y. Gor, M. Thommes, K.A. Cychosz, A.V. Neimark, *J.Carbon*, 2012, 20, 1583–1590.
[16] S. Barbara, InfraredSpectroscopy: *Fundamentals and Applications*, John Wiley & Sons, **2004,** 15-185.
[17] M. Ruszel, B. Grzybowska, M. Laniecki, M. Wojtowski, *Catal. Commun*, **2007**, 8, 1284-1286.
[18] G.O.A Vargas, J.A. De Los Rayes Heredia, M.A Castellanos, L.F. Chen, J.A. Wang, *J.Materials Chemistry and Physics*, **2013**, 139, 125-133.
[19] P. Munusamy, S.Sanghavi,T.Varga,T. Suntharampillai, RSC Advances, **2013**, 4,17, 8421-8430
[20] Y.F. Han, Z. Zhong, K. Ramesh, F. Chen, L. Chen, *J. Phys. Chem. C*, **2007**, 111, 3163-3170.
[21] E.A. Ustinov, D.D. Do, M. Jaroniec. *Appl. Surf. Sci*, **2005**, 252, 1013–1028.
[22] A.V. Neimark, Y. Lin, P.I. Ravikovitch, M. Thommes, Quenched solid density functional theory and pore size analysis of micro-mesoporous carbons, *Carbon*, **2009**, 47, 1617–1628.

AUTHORS' ADDRESSES

1. **Gusliani Eka Putri**
The Institute of Health Science Syedza Saintika
Padang, West Sumatera, Indonesia
E-mail:guslianiekaputri@gmail.com, Mob.No.: 085263640977
2. **Feni Rahayu Gusti**
The Institute of Health Science Syedza Saintika
Padang, West Sumatera, Indonesia
E-mail:fenirahayugusti@gmail.com, Mob.No. : 085263640977
3. **Syukri Arief**
Professor, Department of Chemistry
Faculty of Mathematics and Science, Andalas University,
Padang,West Sumatera, Indonesia
E-mail:syukriarief@gmail.com, Mob.No. : 08126628809
4. **Novesar Jamarun**
Professor, Department of Chemistry
Faculty of Mathematics and Science, Andalas University,
Padang,West Sumatera, Indonesia
E-mail:novesar62@yahoo.com, Mob.No. : 08126713521

5. **Zilfa**
Department of Chemistry
Faculty of Mathematics and Science, Andalas University,
Padang,West Sumatera, Indonesia
E-mail: zilfa_58@yahoo.com, Mob.No. : 081363475422
6. **Upita Septiani**
Department of Chemistry
Faculty of Mathematics and Science, Andalas University,
Padang,West Sumatera, Indonesia
E-mail: upitas@yahoo.com, Mob.No. : 081266622828
7. **Adel Fisli**
Center for Technology of Nuclear Industry Materials,
National Nuclear Energy Agency,
KawasanPuspiptek, Serpong, Indonesia
E-mail: adel@batan.go.id, Mob.No. : 081212635581